Journal of Petroleum Science and Engineering 207 (2021) 109130

Contents lists available at ScienceDirect

Journal of Petroleum Science and Engineering

journal homepage: www.elsevier.com/locate/petrol

The origins of biodegraded oils in sandstone reservoirs in the Termit Basin

Wenqiang Wang[a,b], Tieguan Wang[a], Meijun Li[a,c,*], Fengjun Mao[d], Jiguo Liu[d], Hong Xiao[a], Hongfei Lai[a,e], Xinyu Ai[b]

[a] State Key Laboratory of Petroleum Resources and Prospecting, College of Geosciences, China University of Petroleum, Beijing, 102249, PR China
[b] Research Institute of Yanchang Petroleum (GROUP) Co. Ltd, Xi'an, 710075, PR China
[c] Key Laboratory of Exploration Technologies for Oil and Gas Resources, Ministry of Education, College of Resources and Environment, Yangtze University, Wuhan, 430100, PR China
[d] Research Institute of Petroleum Exploration and Development, PetroChina, Beijing, 100083, PR China
[e] MNR Key Laboratory of Marine Mineral Resource, Guangzhou Marine Geology Survey, Ministry of Natural Resources, Guangzhou, PR China

ARTICLE INFO

Keywords:
Geochemical characteristics
Biodegraded oil
Termit basin
Geological condition

ABSTRACT

Systematic geochemical analysis of 39 crude oils from the Termit Basin, Niger, all belonging to the same oil family, reveals distinct differences in bulk properties and molecular compositions, which were undoubtedly caused by differences in the extent of biodegradation. Various degrees of microbial alteration were identified in crude oils, which were classified as non-, slightly, moderately, or heavily degraded oils, according to their physical properties, bulk chemical compositions, and certain molecular biomarker characteristics. Examination of the possible origins and geological backgrounds of the biodegraded oils shows that reservoirs with deeper burial depths (greater than 1800 m), thicker caprocks (>100 m), relatively higher stratigraphic temperatures (>80 °C), and which have been subject to the influence of silent faults had not suffered significant biodegradation. The burial depth of reservoirs is therefore considered to be the main factor controlling the biodegradation process, and may offset other factors if the depth is sufficient. The Paleogene reservoirs in the Dinga Step-Fault Zone (DSFZ) that meet all of these conditions are therefore dominated by normal oils. Degraded oils of varying degrees are widely distributed in other tectonic units where at least one of these factors is absent. This study may have practical application for further petroleum exploration, prediction of petroleum properties, and the reduction of production risk.

1. Introduction

Most of the world's oil has been adversely affected by biodegradation. It has been estimated that supergiant biodegraded oil reservoirs contain much greater reserves than the largest conventional oil fields in the world (Demaison, 1977). However, the higher costs of recovery and refining of biodegraded oils in shallow reservoirs is an important factor to be considered in planning exploration programs (Jones et al., 2008).

A great deal of work has been done on the physical, chemical, and geological conditions controlling the processes and characteristics of oil biodegradation (e.g., Evans et al., 1971; Milner et al., 1977; Hunt, 1979; Price, 1980; Tissot and Welte, 1984; Wenger et al., 2002). It has been generally accepted that 80 °C is the upper temperature limit for the survival of microorganisms (Brock, 1978; Palmer, 1984; Bernard and Connan, 1992). A number of other factors, such as nutrient supply (Connan, 1984), lithology (McCaffrey et al., 1996; Fredrickson et al., 1997; Krumholz, 2000), and salinity (Grassia et al., 1996), could also have had a significant impact on the scale and degree of biodegradation.

The chemical compositional changes and their sequences in the biodegradation process have been described in detail in previous studies (e.g. Stahl, 1980; Palmer, 1993; Peters et al., 2005). Biodegraded oils generally present with lower API gravity, relatively higher concentrations of asphaltenes + NSO compounds, and higher viscosity and Total Acid Number (TAN) values compared with fresh oils (Tomczyk et al., 2001; Qian et al., 2001; Watson et al., 2002; Barth et al., 2004; Luo and Gu, 2005, 2007). Laboratory and empirical observations have shown that biomarkers can be removed sequentially following a definite priority order (Seifert and Moldowan, 1979; Seifert et al., 1984; Larter et al., 2012). This diagnostic feature provides an effective method for determining the degree of biodegradation of crude oil (Larter et al.,

* Corresponding author. State Key Laboratory of Petroleum Resources and Prospecting, College of Geosciences, China University of Petroleum, Beijing, 102249, PR China.
E-mail address: meijunli@cup.edu.cn (M. Li).

https://doi.org/10.1016/j.petrol.2021.109130
Received 3 February 2021; Received in revised form 21 April 2021; Accepted 18 June 2021
Available online 23 June 2021
0920-4105/

2008).

The Termit Basin is the second largest oil-bearing basin (after the Muglad Basin) in the Central and Western African Rift System (WCARS) (Liu et al., 2012; Lai et al., 2018). Its production capacity has reached nearly 12 × 10^4 barrels of crude oil per day. There have been many recent, detailed studies of the structural evolution of the basin (Fairhead and Binks, 1991; Genik, 1992; Liu et al., 2012), the geological and geochemical characteristics of source rocks (Harouna and Philp, 2012; Li et al., 2018; Xiao et al., 2019; Lai et al., 2019), the occurrence and features of reservoirs (Genik, 1993; Mao et al., 2019), the petroleum accumulation and charging history (Liu et al., 2012, 2019; Lü et al., 2015), the origin and source of petroleum (Genik, 1993; Wan et al., 2014), etc. However, the origins of the biodegraded oils in the area are still poorly understood.

Discovered petroleum in the Termit Basin mainly occurs in Eocene and Upper Cretaceous sandstone reservoirs, with two oil families having been identified and categorized in the basin on the basis of comprehensive oil-oil correlation (Wan et al., 2014). The majority of the oils (oil family I) are sourced from Upper Cretaceous marine shales. Some oils, which occur close to the depocenter of the Dinga Depression (oil family II) are partly sourced from Eocene lacustrine shales (Genik, 1992, 1993; Harouna and Philp, 2012; Wan et al., 2014). Large variations in the biodegradation levels of crude oils have been confirmed by analysis of oils from hundreds of wells spread throughout the Termit Basin.

For this study, 39 oils belonging to the same oil family, with diverse API gravities, were collected from Eocene and Upper Cretaceous sandstones in five main tectonic units of the Termit Basin. The geochemical characteristics and heterogeneity of those oils were determined and described on the basis of standard geochemical experiments. The possible origins of these biodegraded oils are discussed with reference to both the experimental data and the geological factors governing the distribution of the biodegraded oils.

2. Geological setting

As an extensional, asymmetric, Cretaceous-Neogene sedimentary basin, the Termit Basin was deposited above a metamorphic basement which had undergone three tectonic phases (Genik, 1992, 1993, 1993). The wedge of craton which forms the basement was formed during a pre-rift platform phase (approximately 550–130 Ma) (Maurin and Guiraud, 1993).

The syn-rift phase (approximately 130–25.2 Ma) can be subdivided into three stages (Fairhead, 1986). During the Early Cretaceous rifting stage (approximately 130–96 Ma), with the break-up of Gondwana and the opening of the Southern Atlantic (Fairhead and Binks, 1991), a regional NW-SE fault system formed, accompanied by intense rifting (Guiraud et al., 2005). A set of terrigenous stratigraphic successions several kilometers in thickness were deposited during this period (Early Cretaceous). During a thermo-tectonic subsidence stage in the Late Cretaceous (approximately 96–66.5 Ma), regional thermal subsidence coincided with a global rise in sea-levels (Haq et al., 1991) which resulted in widespread marine transgression in the Termit Basin (Reyment and Dingle, 1987; Genik, 1993). The Donga Formation was deposited during this period. The 'Santonian Squeeze', a result of NW-SE compression between the European and African plates in the Santonian period, could have been the cause of the subsequent uplift of the basin (Guiraud and Maurin, 1992; Ziegler, 1990) and the accompanying change from marine sedimentary facies to transitional facies, until the sea-water retreated completely at the end of the late Cretaceous. The Yogou and Madama formations (from bottom to top, respectively) were deposited at this time (Fu et al., 2012). The most recent studies indicate that the discovered oils in the basin are chiefly sourced from the shales and mudstones of the Upper Cretaceous Yogou Formation, which is composed of thick shale and mudstone (Wan et al., 2014; Xiao et al., 2019). The fault system was reactivated along its previous transpressional orientation during the early Paleogene (approximately 66.5–25.2 Ma) which was marked by a collision between the African-Arabian and Eurasian plates (Guiraud et al., 1987). The Paleogene rifting system is characterized by a relative smaller scale, shallower affected depth, and NNW-SSE orientation, which differs from the Late Cretaceous rifting system (Bosworth, 1992; Janssen et al., 1995). During this time, a set of fluvial-deltaic-lacustrine sediments filled within the Paleogene strata, forming the Sokor1, LV, and Sokor2 Formations (from bottom to top, respectively) (Fu et al., 2012). The Eocene Sokor1 Formation is comprised of deltaic-lacustrine sandstone interbedded with shale/-mudstone and is subdivided into five pay zones, labelled the E_5–E_1 sand groups (from deepest to shallowest), which can be identified as the main reservoir of the Termit Basin. The LV and Sokor2 Formations form effective regional cap rocks for the Eocene oil pools (Genik, 1992, 1993, 1993; Lai et al., 2020).

The post-rift phase (approximately 25.2–0 Ma), was the most recent major tectonic stage. This took the form of a long period of thermal tectonic subsidence during which the Neogene and Quaternary, consisting of alluvial-fluvial sediments, were deposited.

The structure of the top surface of the Sokor1 Formation reveals that the Termit Basin comprises ten tectonic units: the Dinga Step-Fault Zone (DSFZ), the Dinga and Moul Depressions, the Araga Graben, the Trakes and Yogou Slopes, the Soudana and Fana Uplifts, and the Eastern and Western Platforms (Tang et al., 2015; Lai et al., 2018; Xiao et al., 2019).

3. Samples and experiments

3.1. Samples

A total of 39 crude oils belonging to oil family I (as defined by Wan et al. (2014)) were collected from the Eocene Sokor1 Formation (36 oils) and Upper Cretaceous Yogou (3 oils) Formation in the Termit Basin. The locations of the samples are shown in Fig. 1 and the bulk properties and group compositions are shown in Table 1.

3.2. Experiments

The conventional geochemical analysis method for crude oils was applied to the samples using the following steps: (1) the crude oils were deasphalted using distilled petroleum ether and then (2) the deasphalted oils were separated into saturated, aromatic and NSO fractions using column chromatography. The column was filled with silica gel/neutral alumina (3:2, w/w), and elution of the fractions was carried out sequentially using petroleum ether, then dichloromethane/petroleum ether (2:1, v/v), and then dichloromethane/methanol (93:7, v/v).

Gas chromatography (GC) analysis of the saturated hydrocarbon fractions was carried out using a Shimadzu GC-2010 gas chromatograph equipped with a Flame Ionization Detector (FID) and an HP-5ms (5%-phenyl)-methylpolysiloxane fused silica capillary column 30 m in length. Helium was used as the carrier gas. The GC oven temperature was programed at 100 °C/min, ramped to 300 °C at 4 °C/min, and finally held at that temperature for 25mins.

An Agilent 6890 gas chromatograph and matched Agilent 5975i mass spectrometer (GC–MS) was used for biomarker analysis of the saturated and aromatic hydrocarbon fractions. An HP-5ms fused silica capillary column (60 m × 0.25 mm i.d. with a 0.25 μm film) was used with Helium as the carrier gas. The programmed temperature for detection of saturated hydrocarbon fractions was set at 50 °C, then ramped at 20 °C/min to 120 °C, then at 3 °C/min until the temperature reached 310 °C, where it was held for 25 min. For the aromatic hydrocarbon fractions, the heating rate was constant at 3 °C/min throughout the process until the temperature reached 310 °C, where it was held for 16 min. The MS was operated in both full scan mode (m/z 50–570) and selected ion monitoring (SIM) mode, with an ionization energy of 70 eV.

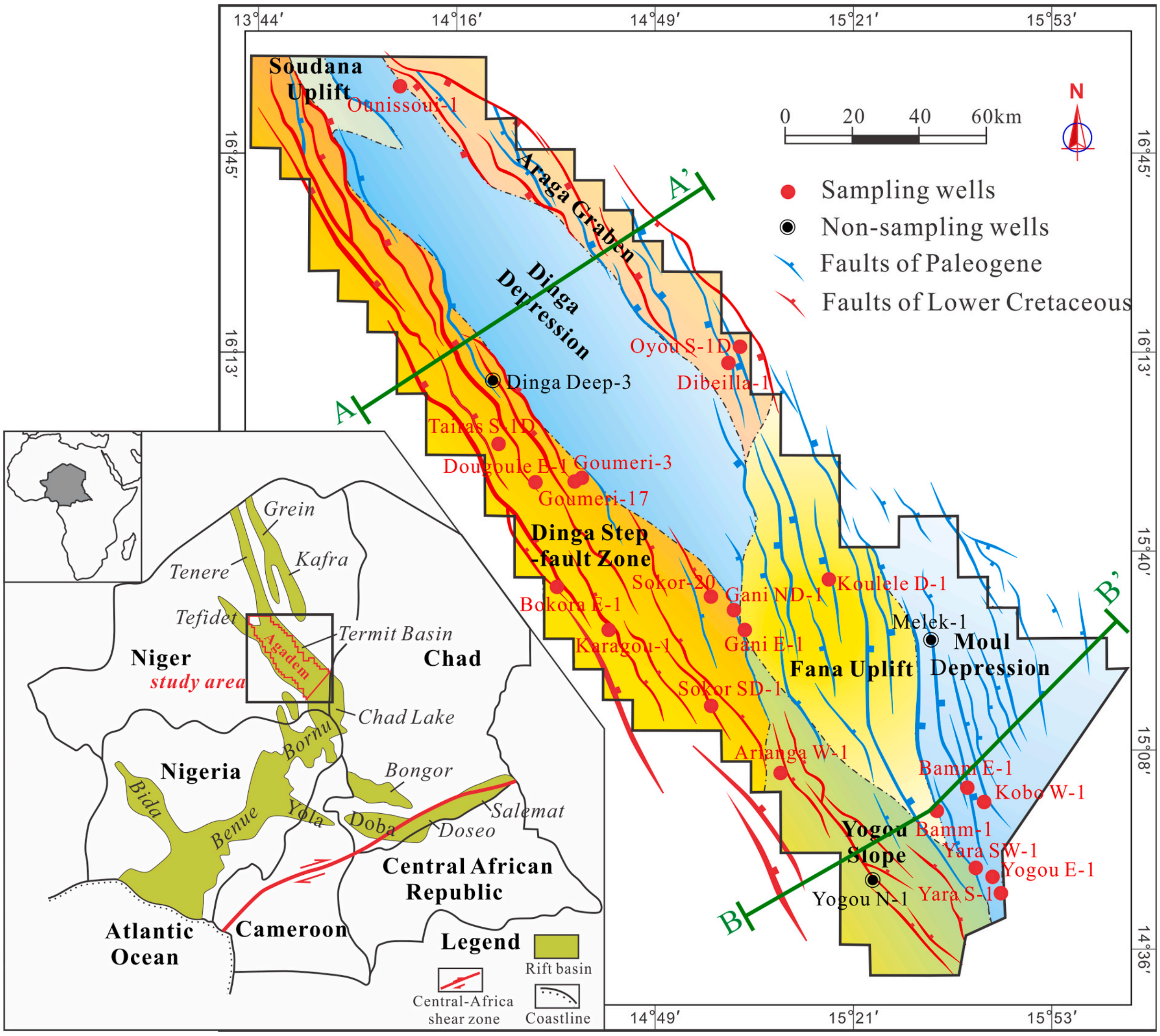

Fig. 1. Map of geographic location and schematic structures of the Termit Basin, Niger (modified after Genik, 1993).

4. Results and discussion

4.1. Physical properties and bulk compositions

For crude oils from the same source kitchen, heterogeneity of fluid properties and geochemical characteristics are mainly the results of secondary alteration processes, among which biodegradation is commonly the predominant process (Horstad and Larter, 1997; Larter et al., 2008, 2012).

The API gravities and bulk compositions of the crude oils from oil family I in the Termit Basin were quantitively analyzed. The characteristics of bulk composition, as set out in Table 1, occurred within the ranges 16.5° to 39.8° for API gravities and 1.4 to 9.4 for saturated/aromatic hydrocarbon fraction values (Sat/Aro). This variability clearly correlated with the areal distribution of the samples and also exhibited saltation in geological conditions within the same tectonic unit. For example, the values of both API gravities and Sat/Aro are relatively high in the DSFZ, reaching mean values of 30.7° and 5.4, respectively, but drop to 21.8° and 3.6 in the Moul Depression (Table 1 and Fig. 3). Also, the Sat/Aro values generally increase with increasing reservoir burial depth, particularly in the three oils from the Yogou Formation (and some other samples) (Table 1). Furthermore, one oil sample (from Well Bokora E−1 1307.7–1310.2 m, E_1) with heavy oil characteristics contains higher quantities of asphaltenes + NSO fractions (Fig. 2) and has a relatively lower API gravity than oils from the DSFZ, which are mostly normal. On the other hand, the relatively high viscosities and TAN values of several of the crude oils suggests that secondary alteration occurred to varying degrees in the reservoirs in the Termit Basin. The highest values for viscosity and TAN were found in the Moul Depression, up to 580.5 mPa s and 1.45 mg KOH/g, respectively. This may represent strong additional evidence for gas/water washing, or for biodegradation while the oil was in a mature or highly-mature stage (Peters et al., 2005; Dou et al., 2008; Li et al., 2010). Finally, a negative correlation between the asphaltene + NSO fractions and the API gravities of the crude oils can be clearly observed in Fig. 3.

The absence of evidence of water washing in bulk compositions, such as increased Sat/Aro (Bailey et al., 1973; Kuo, 1994; Hemptinne et al., 2001; Chang et al., 2017), combined with the high acidity of the oils (Cheng et al., 2010), signifies that biodegradation rather than water washing was the predominant factor controlling the origins of transformed oils in the Termit Basin. Degrees of biodegradation vary with the differences in geological conditions among the tectonic units, just as normal oil predominates in the DSFZ and heavy oils in the Moul Depression and the Fana Uplift. Furthermore, geological inconsistencies within the same tectonic unit have also contributed to variations in the degrees of biodegradation.

Table 1
Oil samples with bulk composition and physical properties.

Tectonic unit	Well No	Depth (m)	Pay zone	API°	Sat(wt%)	Aro(wt%)	Resin (wt %)	Asphaltene (wt %)	Sat/Aro	BD*
raga Graben	Dibeilla-1	1313.6–1318.0	E_2	18.6	63.8	20.5	11.8	3.9	3.1	M
	Dibeilla-1	1458.5–1464.5	E_3	26.4	71.1	16.6	8.6	3.7	4.3	L
	Dibeilla-1	1565.0–1574.0	E_4	26.8	69.5	13.9	7.7	8.9	5.0	L
	Dibeilla-1	1706.0–1714.0	E_5	20.5	55.5	22.6	15.8	6.1	2.5	M
	Oyou S-1D	1043.0–1050.0	E_2	20.5	60.3	20.9	15.6	3.2	2.9	H
	Ounissoui-1	1243.5–1249.5	E_4	20.7	60.6	22.1	12.7	4.6	2.7	M
Dinga Step-Fault Zone	Tairas S-1D	2441.5–2447.0	E_2	38.6	71.2	13.5	11.5	3.8	5.3	N
	Goumeri-17	2637.0–2642.0	E_3	33.6	66.5	14.6	6.6	12.3	4.5	N
	Sokor-20	2014.0–2026.0	E_2	29.9	81.3	8.7	9.1	0.9	9.4	N
	Karagou-1	1763.0–1765.1	E_2	31.3	63.6	23.8	10.2	2.4	2.7	N
	Karagou-1	2047.2–2059.2	E_4	31.5	67.0	17.4	11.8	3.8	3.9	N
	Dougoule E−1	2012.9–2026.5	E_2	n.d.	69.7	13.8	11.0	5.5	5.1	N
	Dougoule E−1	2032.4–2035.9	E_2	n.d.	72.1	14.6	10.6	2.7	4.9	N
	Dougoule E−1	2164.7–2185.4	E_3	33	70.1	14.8	13.4	1.7	4.7	N
	Dougoule E−1	2207.6–2209.4	E_3	n.d.	69.2	14.2	9.9	6.7	4.9	N
	Dougoule E−1	2421.6–2425.7	E_4	33.2	71.1	13.6	9.4	5.9	5.2	N
	Dougoule E−1	2452.0–2454.3	E_4	32.7	69.1	14.3	9.2	7.4	4.8	N
	Sokor SD-1	3099.9–3103.0	Yogou	38	84.1	9.4	5.3	1.2	9.0	N
	Sokor SD-1	3245.6–3255.1	Yogou	39.8	80.7	9.0	6.6	3.6	8.9	N
	Sokor SD-1	3218.2–3221.0	Yogou	39.5	80.4	11.0	6.4	2.3	7.3	N
	Sokor SD-1	2048.9–2052.0	E_3	29.4	62.1	17.3	9.9	10.6	3.6	N
	Bokora E−1	1307.7–1310.2	E_1	17.1	61.9	17.8	15.6	4.7	3.5	M
	Bokora E−1	1357.0–1358.6	E_2	26.3	67.1	20.6	10.7	1.7	3.3	L
	Gani ND-1	1414.9–1421.1	E_1	23.9	67.3	23.3	9.0	0.5	2.9	M
	Goumeri-3	2382.7–2410.0	E_1	29.2	71.0	13.9	9.5	5.6	5.1	N
	Goumeri-3	2568.5–2571.8	E_2	30	70.2	12.5	10.2	7.1	5.6	N
	Goumeri-3	2690.0–2693.0	E_3	27.2	74.5	9.9	7.3	8.3	7.5	N
	Goumeri-3	2720.6–2725.5	E_3	34.6	76.0	10.7	8.2	5.1	7.1	N
Fana Uplift	Gani E−1	1478.2–1482.8	E_1	24	73.4	14.9	8.5	3.2	4.9	M
	Gani E−1	1500.7–1511.2	E_1	30.2	73.0	13.5	9.8	3.7	5.4	L
	Koulele D-1	1329.0–1335.0	E_2	16.2	46.7	33.6	18.2	1.5	1.4	M
Moul Depression	Kobo W-1	1598.7–1602.0	E_1	n.d.	59.4	15.3	17.1	8.2	3.9	M
	Bamm E−1	1637.1–1648.1	E_1	26.6	75.8	13.2	8.8	2.2	5.7	M
	Yara SW-1	1419.6–1422.0	E_2	n.d.	56.3	18.5	24.1	1.1	3.0	M
	Yara SW-1	1496.7–1501.0	E_3	20.2	61.5	22.3	13.2	2.9	2.8	M
	Yara S-1	1269.7–1271.6	E_1	20.3	60.3	20.5	16.5	2.7	2.9	H
	Yogou E−1	1130.4–1134.2	E_0	21.4	61.3	17.0	19.8	2.0	3.6	H
	Bamm-1	1520.2–1524.6	E_2	20.7	56.4	17.3	15.8	10.5	3.3	M
Yogou Slope	Arianga W-1	1330.3–1341.6	E_2	21.2	56.8	20.4	20.4	2.5	2.8	M

Notes: BD* = Biodegradation Degree; N=Non-biodegraded oil; L = Lightly biodegraded oil; M = Moderately biodegraded oil; H=Heavily biodegraded oil.

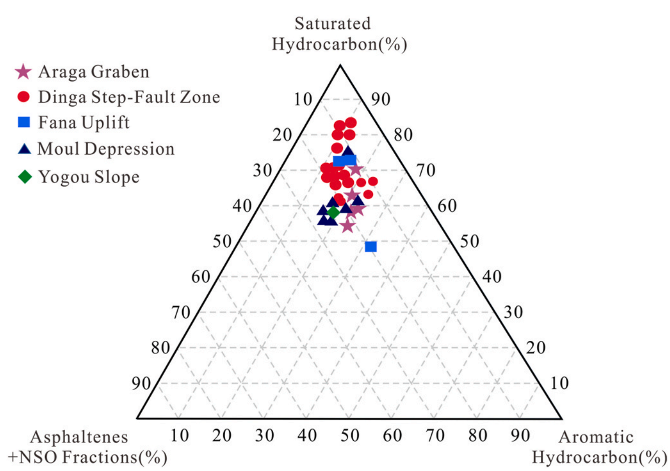

Fig. 2. Ternary diagram showing the relative abundance of saturated, aromatic, and asphaltenes + NSO fractions in oils from the Termit Basin.

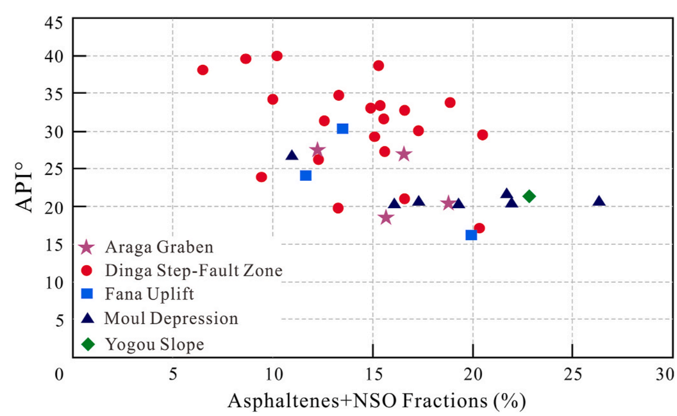

Fig. 3. Cross plots of API gravity vs. asphaltenes + NSO fractions content of oil samples from the Termit Basin.

4.2. The distribution of normal alkanes and acyclic isoprenoids

Larter (2012) offered a summary of preceding studies of biodegradation (Winters and William, 1969; Volkman et al., 1983; Connon, 1984; Head et al., 2003; Peters et al., 2005), concluding that *n*-alkanes tend to be preferentially attacked, followed by branched saturates, because of the shielding from bacterial attack provided by methyl groups. Different levels of biodegradation were variously represented on gas chromatograms (GC), manifested in the abundance and distribution patterns of *n*-alkanes series and acyclic isoprenoids as well as the characteristics of baselines. Representative Gas Chromatograms showing varying degrees of biodegradation of oil samples are shown in Fig. 4. These are limited to the range of C_{13}+ because of the evaporation of gaseous alkanes and gasoline.

Incremental removal of *n*-alkanes and acyclic isoprenoids is revealed, in combination with an Unresolved Complex Mixture (UCM)

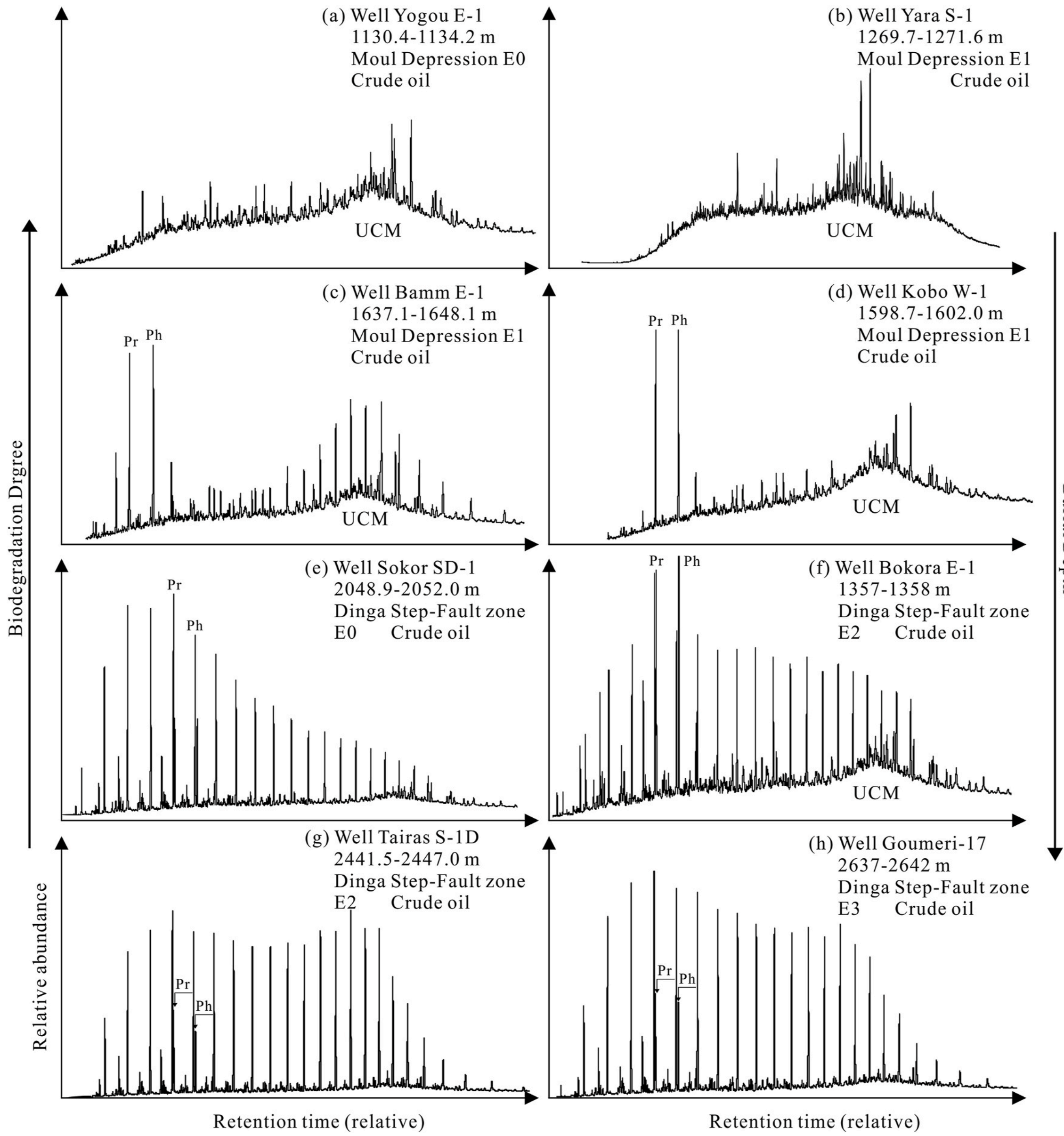

Fig. 4. Gas chromatograms showing the distribution of normal alkanes and acyclic isoprenoids.

'hump', as the burial depth of accumulated oil becomes shallower. The oils were divided into four groups (non-biodegraded, slightly biodegraded, moderately biodegraded, and heavily biodegraded) based on the foregoing features. For example, two non-biodegraded oils discovered in deep-buried reservoirs are represented as dominant pristine *n*-alkane series (C_{13}–C_{36}) with a straight baseline (Fig. 4 g and h). As biodegradation levels increase, the relative abundance of acyclic isoprenoids (e.g., pristane and phytane) in the Gas Chromatograms increases relative to the *n*-alkane series because of their higher resistance to biodegradation. Samples with this characteristic were classified as 'slightly biodegraded' oils (Fig. 4 e and f). As the degree of biodegradation increases, the *n*-alkane series essentially disappears while the pristane (Pr)/phytane (Ph) alkanes partly remain. The emergence of the UCM 'hump' and a raised GC baseline result from the occurrence of a series of unrecognizable lower abundance compounds which are produced by the (usually moderate) biodegradation of high abundance compounds (Fig. 4 c and d). Heavily biodegraded oils consistently demonstrate both progressive intensification of the UCM 'hump' and a rising baseline accompanied by a depletion of acyclic isoprenoids (Fig. 4 a and b). Moreover, the API gravity of crude oil generally decreases linearly with aggravation of biodegradation.

The parameter of pristine-to-nC_{17} alkane vs. phytane-to-nC_{18} alkane ratios has been applied extensively as an indicator of biodegradation degree for slightly to moderately biodegraded oils (Fig. 5). Varying levels of biodegradation had occurred in the samples in this study that were sourced from mixed organic matter deposited in a transitional environment. The areal distribution of biodegradation also shows clear differentiation. Non- and slightly biodegraded oils primarily accumulated in the DSFZ, but two samples with relatively shallower burial depths had also suffered slight biodegradation (Fig. 5). Moderately and heavily biodegraded oils are more common in the Moul Depression and the Fana Uplift, as shown in Figs.3 and 8, and Fig. 9.

4.3. *Aromatic steroids*

Triaromatic steroids (TAS) are fairly resistant to bacterial attack and are detectable even in severely biodegraded oils (Rubinstein et al., 1977; Larter et al., 2012; Yang et al., 2015). Triaromatic steroids are widely used for ascertaining oil-oil relationships in highly mature or severely biodegraded crude oils. Because of their high stability they are also used

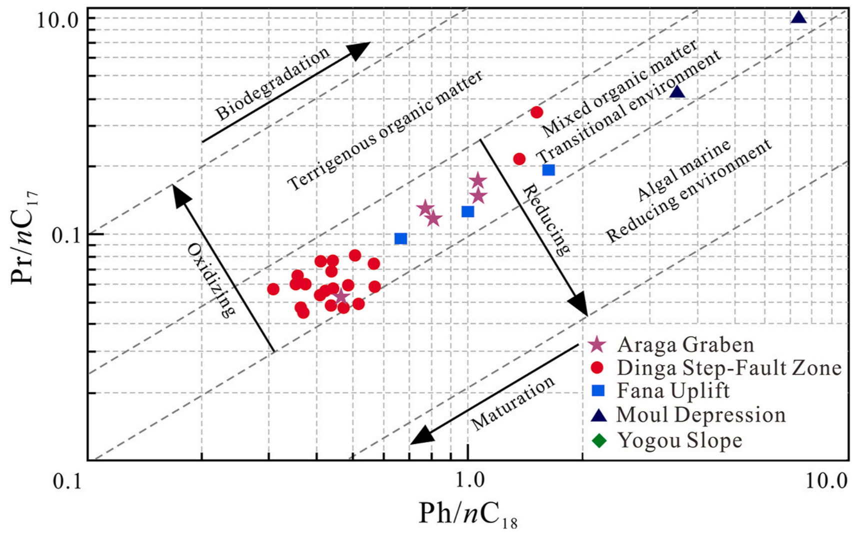

Fig. 5. Cross plots of pristine-to-nC_{17} alkane (Pr/nC_{17}) vs. phytane-to-nC_{18} alkane (Ph/nC_{18}) of crude oils from the Termit Basin (after Shanmugam, 1985).

to estimate thermal maturity (Fig. 6). Triaromatic steroids are identified by conventional GC–MS (*m/z* 231) analysis of aromatic fractions. However, the co-elution of C_{26} TAS 20R and C_{27} TAS 20S is a barrier to widespread application of this method (Yang et al., 2015; Zhang et al., 2016, 2016b) and will remain so until an effective and straightforward method is found to determine the relative abundance of each of these compounds.

Oil-oil correlation in the Termit Basin can be effectively illustrated in a ternary diagram of triaromatic steroids (Fig. 7). The crude oils from the Termit Basin all exhibit a highly consistent distribution of triaromatic steroids and the content of C_{28} TAS generally reaches 70.01% on average. This result confirms that the sampled oils belong to the same oil family. Furthermore, the biodegradation process may be the key factor controlling the differentiation of physical properties, even at a molecular level, in crude oils from the Termit Basin.

4.4. Geological conditions for oil biodegradation

As described above, the differences between these oils, which are all from oil family I, are mainly caused by their varying degrees of biodegradation. The geological conditions which control the heterogeneity of biodegradation are therefore of considerable significance.

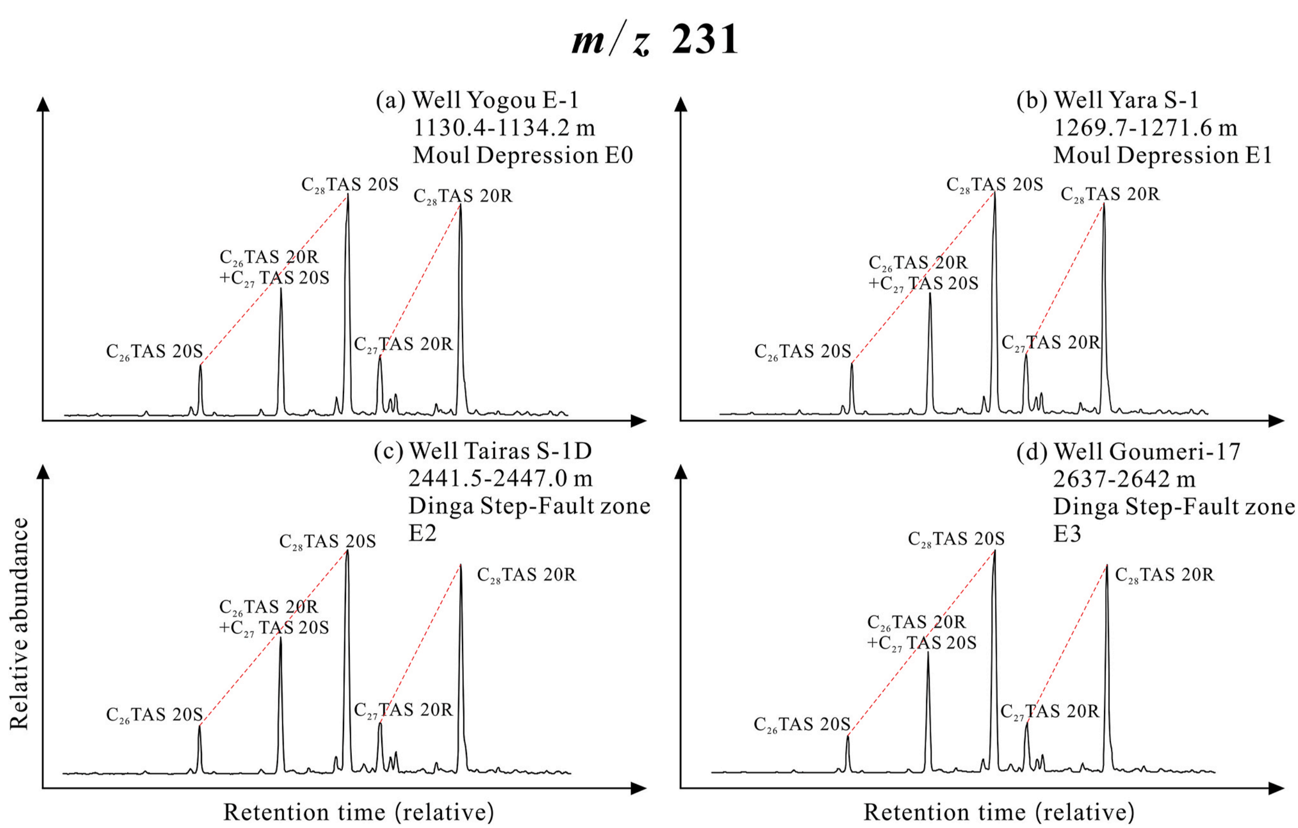

Fig. 6. Mass chromatograms of *m/z* 231 (aromatic hydrocarbons) showing the distribution of triaromatic steroids.

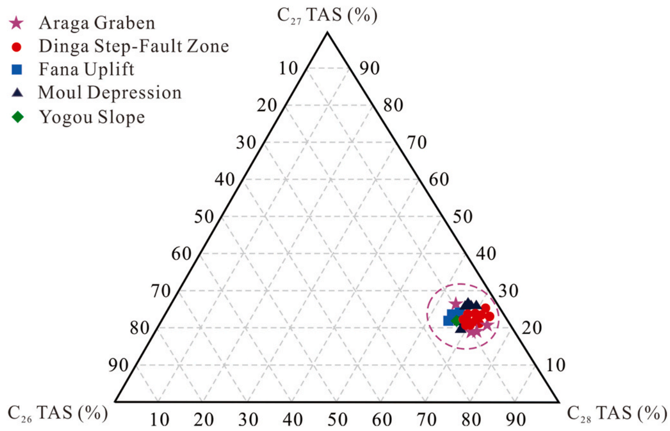

Fig. 7. Ternary diagram showing the relative compositions of C_{26}, C_{27} and C_{28} TAS of crude oils from the Termit Basin.

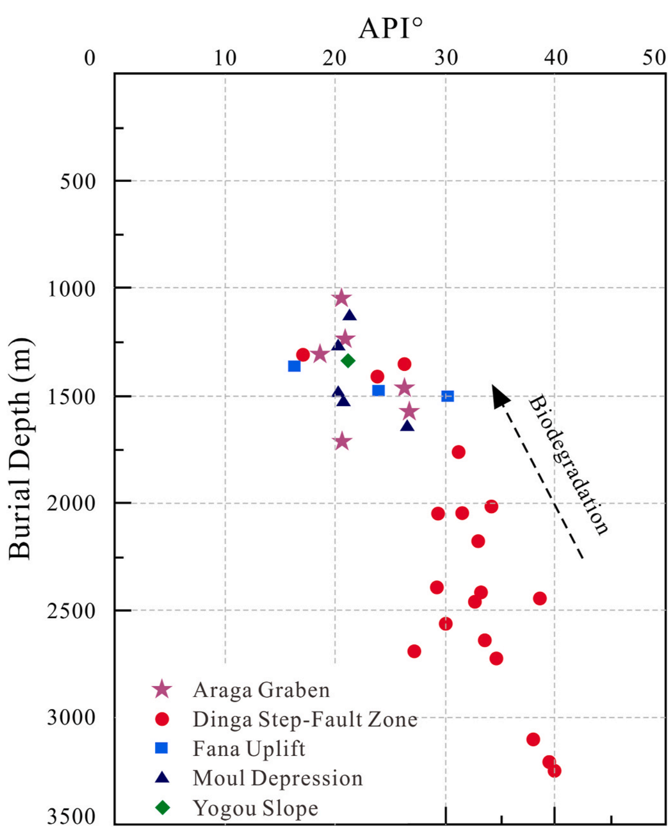

Fig. 8. Relationship of API gravity as a function of burial depth for crude oils in the Termit Basin.

4.4.1. Burial depth

In general, the burial depths of reservoirs are in close positive correlation with reservoir temperatures and the ability of meteoric water to permeate the reservoir. The sterilized and hypoxic reservoir conditions, with fewer nutrients, that usually occur at relatively greater burial depths prevent microbes thriving by inhibiting the aerobic and anaerobic processes that metabolize crude oil (Connon, 1984; Wenger et al., 2002; Yang et al., 2019).

This rule applies equally in the Termit Basin, as revealed in Fig. 8. The heterogeneity of burial depths of reservoirs in the different tectonic units correlates clearly with the API gravities of oils trapped in the respective units. Most Paleogene reservoirs in the Termit Basin have relatively shallow burial depths (Table 1). For instance, the mean burial depths of reservoirs in the Moul Depression and the Araga Graben are 1420.9 m and 1514.2 m, respectively, but, in the DSFZ, depths reach 2398.7 m. Furthermore, almost all crude oils pooled at depths greater than 1800 m present as non- and slightly biodegraded and have relatively high API gravities (even higher than 35°). Crude oils accumulated in shallower strata ($<$ 1500 m) often show lower API gravities accompanied by poor fluidity. The API gravity of oil clearly responds to secondary alteration, particularly biodegradation.

The relationship between the biodegradation levels of crude oils and their burial depths is evident in Fig. 9. Almost all non- and slightly biodegraded oils are concentrated in the DSFZ, with relatively lowe Pr/nC$_{17}$ and Ph/nC$_{18}$ values (0.43 and 0.60, respectively), due to the relatively deep burial of the reservoir from a plane perspective. However, the significant phenomenon is that three samples (from Well Bokora E−1 at 1307.7–1310.2 m and 1357.0–1358.6 m, and from Well Gani ND-1 at 1414.9–1421.1 m) exhibit inconsonant geochemical characteristics. These three samples have API gravities of 17.1, 26.3, and 23.9, respectively, and Ph/nC$_{18}$ values of 3.48, 2.17, and 8.21. The relative shallower burial depths of these samples compared with the other oils from the DSFZ may explain this inconsistency. The biodegradation degrees of oils from other tectonic units buried within the range 1800–1000 m also show great differences. Almost all of these oils have experienced at least moderate biodegradation, with relatively higher Pr/nC$_{17}$ and Ph/nC$_{18}$ values (mean value of 2.09 and 4.22, respectively). The moderately biodegraded oils collected from the Moul Depression show the highest values for Pr/nC$_{17}$ and Ph/nC$_{18}$ (mean value of 4.43 and 9.07, respectively). In general, 1800 m is an important burial depth threshold in the Termit Basin. None of the oils discovered at greater depths have undergone severe microbial attack, while the oils discovered within a depth range of 1800–1000 m are all biodegraded to varying degrees. It is clear, therefore, that the burial depth of reservoirs is the most important factor influencing biodegradation and that burial depth may offset other factors if the depth is sufficient.

4.4.2. Stratigraphic temperature

Stratigraphic temperature is another primary controlling factor for degree of biodegradation (Connan, 1984). Excessive reservoir temperatures may reduce microbial activity until biodegradation rates effectively sink to zero at around 80 °C (Bernard and Connan, 1992; Palmer, 1993; Larter et al., 2003; Head et al., 2003). It can be assumed that the significant differences in burial depth of the Paleogene reservoirs between the different tectonic units are responsible for the heterogeneity of stratigraphic temperatures.

Three representative wells: Wells Dinga Deep-3 (located in the DSFZ), Melek-1 (located in the Fana Uplift) and Yogou N-1 (located in the Yogou Slope), were reconstructed in 1-D burial-thermal models by Lai et al. (2019) and Lai et al. (2020). The thermal histories of the wells were extracted and are shown in Fig. 10. The average surface temperature was set at 20 °C. The figure clearly illustrates the temperature evolution of the Sokor1 Formation, which represents the major reservoir, since oil charging began at *c.* 13 Ma (Liu et al., 2019), with temperatures in the range of 94–103 °C (Dinga Deep-3), 76–82 °C (Melek-1), and 74–79 °C (Yogou N-1). Similar reservoir temperatures, coupled with burial depths, are characterized by the Fana Uplift and the Yogou Slope. Maintenance of suitable stratigraphic temperatures for microbial activity over long periods is one of the reasons why crude oils suffered biodegradation in the southern part of the Termit Basin. In contrast, the DSFZ has experienced a pasteurizing temperature exceeding the upper limit for biodegradation by nearly 20 °C since the beginning of oil charging, which has been conducive to oil quality stabilization.

4.4.3. Fault architectures

Faults may not only play a role in connecting source kitchens and reservoirs but may also decrease the dynamic sealing capacity of traps. As mentioned, the Termit Basin is characterized by two distinct rifting systems, distinguished in terms of their controlling factors and periods of

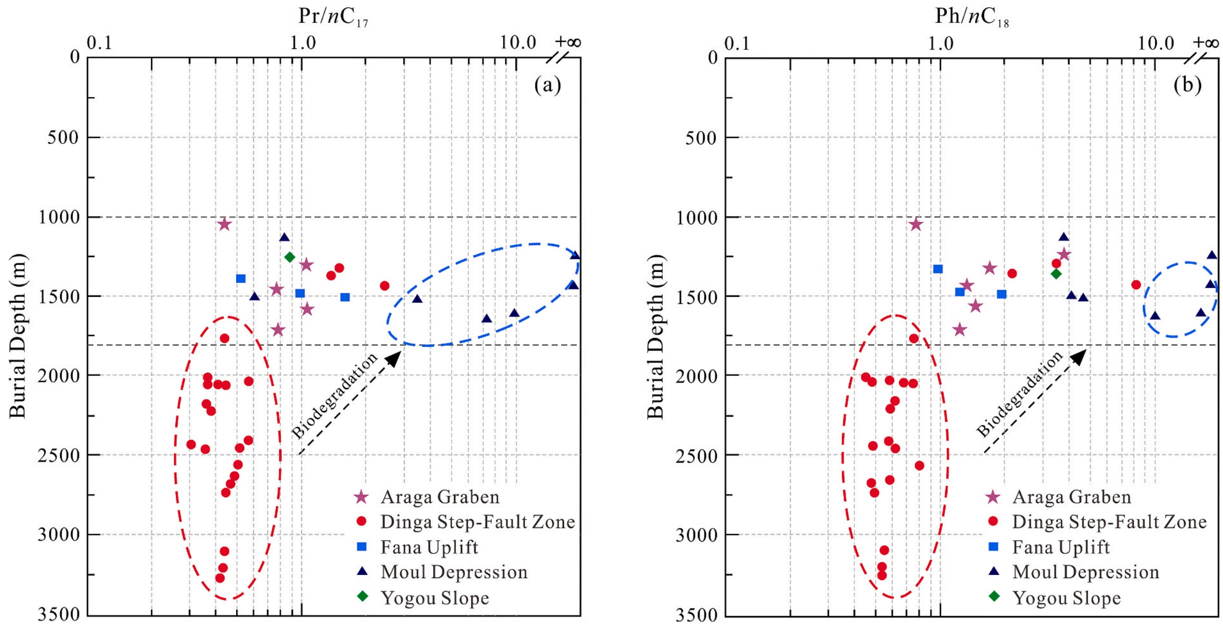

Fig. 9. Variations of Pritane-to-nC_{17} alkane (Pr/nC_{17}) (a) and Phytane-to-nC_{18} (Ph/nC_{18}) (b) with burial depth of crude oils in the Termit Basin.

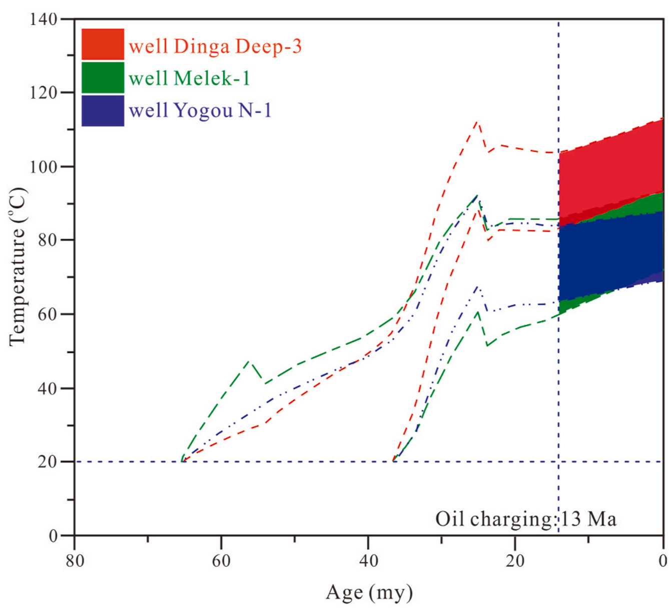

Fig. 10. Temperature correlation diagram of Sokor1 Fm. with different tectonic units in the Termit Basin (modified from Lai et al., 2019; Lai et al., 2020). The well locations are shown in Fig. 1.

activity. The early deep faults, which were controlled by the break-up of Gondwana during the Early Cretaceous, are reflected as NE-SW orthogonal extension at the major margins of the Termit Baisn (other than the southeast). The rift axis subsequently gradually changed to oblique extension during the Paleogene and this process was responsible for the reactivation of early deep faults and the development of associated late-derived faults. These late-derived faults developed throughout the Termit Basin, especially in the Moul Depression and the Fana Uplift (Fig. 1). The differences in fault distribution and activity characteristics are therefore most evident between the northern and southern parts of the Termit Basin (Fig. 11). Compared with the Early Cretaceous faults, Paleogene faults present on a smaller fault scale, with larger fault distances and extension lengths, denser fault numbers, and weaker activity (Liu et al., 2012). The homogenization temperatures of aqueous inclusions in the Paleogene reservoirs were measured by Liu et al. (2019). The results show that the major charging period occurred immediately after the peak of Paleogene rifting, which ended at 25.2 Ma. Thus, it can be inferred that emerging late-derived faults may have posed a significant threat to the sealing capacity of traps. The long-silent Cretaceous rifting in the DSFZ may have played an important role in oil accumulation, acting both as an intermediary between source kitchen and traps and also as a protector of accumulating and accumulated oil due to the comparatively weak activity since the beginning of oil charging in the Termit Basin.

4.4.4. Thickness of regional cap formation

Sealing by effective cap rocks is one of the key factors for the preservation of subsurface crude oil (Hunt, 1979). As long as the lithology is consistent, sealing improves progressively with increasing thickness (Lü et al., 2017). The LV Formation, which is overlapped adjacent to the sandstone reservoir, serves as the regional cap rock (Lai et al., 2020). It is dominated by thick lacustrine shale and/or mudstone and presents obvious variations in thickness. All of the strata thickness data and some of the well locations referenced in this study are drawn from an unpublished internal report of China National Petroleum Corporation. The LV formation is at its greatest thickness in the DSFZ, particularly in the center and north, where it reaches 210 m and 140 m, respectively (Fig. 12). This great thickness of caprock has effectively prevented the entry of oxygen (free and/or combined) and nutrients dissolved in meteoric water, thus reducing the likelihood of biodegradation occurring. Generally, oils in regions with caprocks of thickness greater than 100 m have not been affected by biodegradation (Fig. 12). The relatively thicker caprock in the DSFZ may partly explain the occurrence of non- and slightly biodegraded oils in that area.

In contrast, crude oils in regions with relatively thinner caprocks, such as the Moul Depression, the Fana Uplift and the Araga Graben, have generally suffered moderate to heavy biodegradation. For instance, in Well Yogou E−1 which is located in the south of the Moul Depression, the thickness of the LV formation is less than 80 m. Crude oil discovered here shows heavy biodegradation both in GC analysis and also according to several biomarker parameters (Figs. 4 and 9).

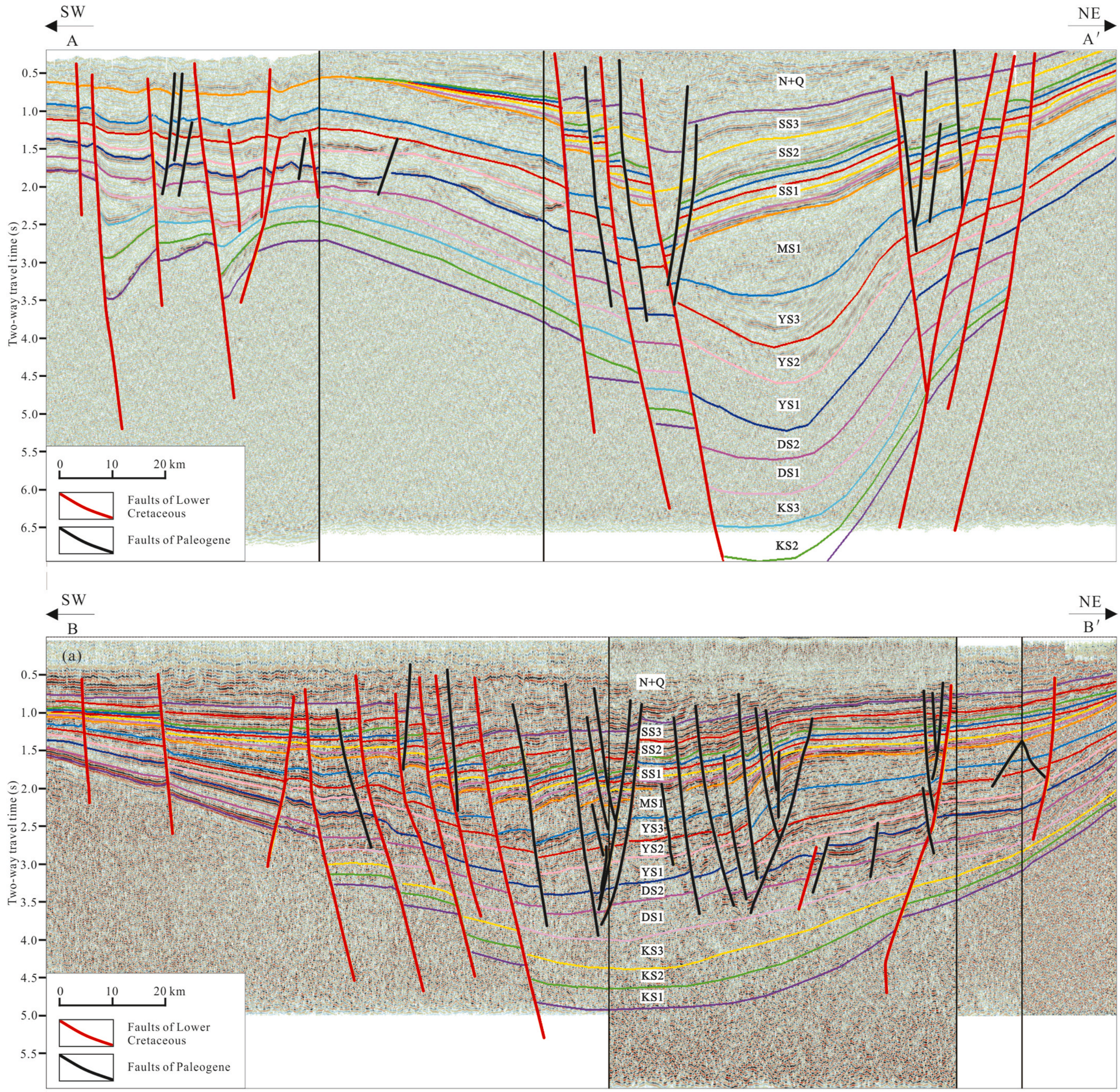

Fig. 11. Regional seismic section across the northern and southern part of the Termit Basin. The location of seismic sections AA′ and BB′ are shown in Fig. 1, respectively.

5. Conclusions

In this study, 39 genetically related oil samples were analyzed to determine the geochemical characteristics and possible origins of crude oils in the Termit Basin according to their relative degrees of biodegradation. The oils were classified into non-biodegraded, slightly biodegraded, moderately biodegraded, and heavily biodegraded oil according to analysis of their physical properties, bulk compositions, and molecular markers. Compositional differences between the oils were mostly attributable to biodegradation. The distribution of biodegraded crude oils is characterized by the concentration of non- and slightly biodegraded oils in the DSFZ and the widespread occurrence of moderately biodegraded oils in other tectonic units, particularly in the Moul Depression and the Fana Uplift.

Burial depth is still the key factor controlling the level of degradation. Burial depth of 1800 m is a critical threshold, beyond which depth can counteract the effects of other geological conditions to inhibit biodegradation. The average burial depth of Paleogene sandstone reservoirs in the DSFZ reaches nearly 2400 m, which is the most plausible explanation for the differences in biodegradation levels in oils between this area and others. The long-term sterilizing temperatures of Paleogene reservoirs in the DSFZ has limited the activity of microbial organisms since the beginning of oil charging. In the Fana Uplift and the Moul Depression, where active derived faults are more developed, there is a greater risk of biodegradation. In addition, caprocks with a thickness of greater than 100 m may have effectively prevented the occurrence of

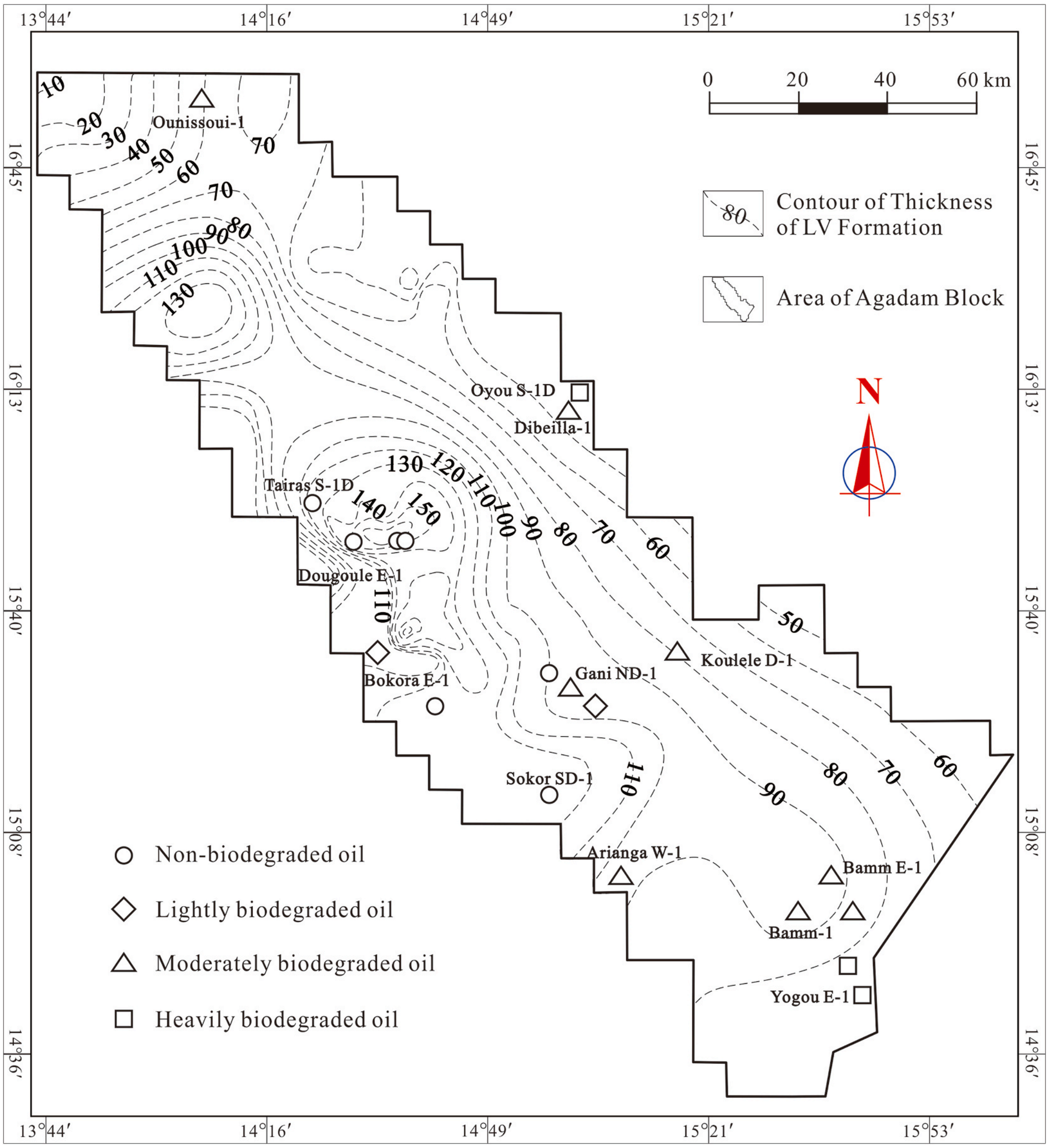

Fig. 12. Isogram showing the thickness of the LV Formation in the Termit Basin (modified after internal report from the Research Institute of Petroleum Exploration and Development, PetroChina, 2018).

biodegradation in parts of the Termit Basin.

Credit author statement

Wenqiang Wang: Ideas provided, Writing, Manuscript Edited. Meijun Li: Manuscript revised. Tieguan Wang: Manuscript revised. Fengjun Mao: Collected samples and materials. Jiguo Liu: Collected samples and materials. Hong Xiao: Conducted experiments and analyzed data. Hongfei Lai: Conducted experiments and analyzed data. Xinyu Ai: Conducted experiments and analyzed data.

Declaration of competing interest

The authors declare that they have no known competing financial interests or personal relationships that could have appeared to influence the work reported in this paper.

Acknowledgements

This study was sponsored by China National Key Project (2016ZX05029). We thank Dr. Dingsheng Cheng for samples providing and data supporting. We appreciate the Research Institute of Petroleum Exploration and Development, PetroChina for the permission to publish this manuscript, and are also grateful for the assistance of Shengbao Shi and Lei Zhu for the geochemical analyses of all selected oils. The authors thank anonymous editors and reviewers for the constructive suggestions and comments.

References

Bailey, N., Krouse, H., Evens, C., Rogers, M., 1973. Alteration of crude oil by waters and bacteria – evidence from Geochemical and isotope studies. AAPG (Am. Assoc. Pet. Geol.) Bull. 57, 1276–1290.

Barth, T., Høiland, S., Fotland, P., Askvik, K.M., Pedersen, B.S., Borgund, A.E., 2004. Acidic compounds in biodegraded petroleum. Org. Geochem. 35, 1513–1525.

Bernard, F.P., Connan, J., 1992. Indigenous microorganisms in connate waters of many oil fields: a new tool in exploration and production techniques. Spe 24811. In: 67th Annual Technical Conference and Exhibition of the Society of Petroleum Engineers, Washington, DC, October 1992, pp. 467–476.

Bosworth, W., 1992. Mesozoic and early tertiary rift tectonics in east africa. Tectonophysics 209, 115–137.

Brock, T.D., 1978. Thermophilic Microorganisms and Life at High Temperatures. Springer-Verlag, Berlin.

Chang, X., Zhao, W., Xu, Y., Wang, T., Cui, J., 2017. Biodegradation and water washing effects on oil during water flooding. Oil Gas Geol. 38, 617–625 (in Chinese with English abstract).

Cheng, D., Dou, L., Wan, L., Shi, Q., 2010. Formation mechanism analysis of Sudan high acidity oils by electrospray ionization fourier transform ion cyclotron resonance mass spectrometry. Acta Petrol. Sin. 26, 1303–1312 (in Chinese with English abstract).

Connan, J., 1984. Biodegradation of crude oils in reservoirs. In: Brooks and Welte (Ed.), Advances in Petroleum Geochemistry, vol. 1. Academic Press, London, pp. 299–335.

Demaison, G.J., 1977. Tar sands and supergiant oil fields. AAPG (Am. Assoc. Pet. Geol.) Bull. 61, 1950–1961.

Dou, L., Cheng, D., Li, M., Xiao, K., Shi, B., Li, Z., 2008. Unusual high acidity oils from the great palogue field, melut basin, Sudan. Org. Geochem. 39, 210–231.

Evans, C., Rogers, M., Bailey, N.J., 1971. Evolution and alteration of petroleum in Western Canada. Chem. Geol. 8, 147–170.

Fairhead, J., 1986. Geophysical controls on sedimentation within the African Rift systems. Geological Society, London, Special Publications 25, 19–27.

Fairhead, J.D., Binks, R.M., 1991. Differential opening of the central and south atlantic oceans and the opening of the west African Rift system. Tectonophysics 187, 191–203.

Fredrickson, J.K., McKinley, J.P., Bjornstad, B.N., Long, P.E., Ringelberg, D.B., White, D. C., Krumholz, L.R., Suflita, J.M., Colwell, F.S., Lehman, R.M., Phelps, T.C., Onstott, T.C., 1997. Pore-size constrains on the activity and survival of subsurface bacteria in a late cretaceous shale-sandstone sequence, northwestern New Mexico. Geomicrobiol. J. 14, 183–202.

Fu, J., Sun, Z., Liu, K., 2012. The study on sequence stratigraphy and sedimentary systems of Paleogene in Agadem Block, Niger. Earth Sci. Front. 19, 58–67 (in Chinese with English abstract).

Genik, G.J., 1992. Regional framework, structural and petroleum aspects of rift basins in Niger, Chad and the Central African Republic (C.A.R.). Tectonophysics 213, 169–185.

Genik, G.J., 1993. Petroleum geology of Cretaceous-Tertiary rift basins in Niger, Chad, and Central African Republic. AAPG (Am. Assoc. Pet. Geol.) Bull. 77, 1405–1434.

Grassia, G.S., McLean, K.M., Glénat, P., Bauld, J., Sheehy, A.J., 1996. A systematic survey for thermophilic fermentative bacteria and archaea in high temperature petroleum reservoirs. FEMS Microbiol. Ecol. 21, 47–58.

Guiraud, R., Maurin, J.C., 1992. Early cretaceous rifts of western and central africa: an overview. Tectonophysics 213, 153–168.

Guiraud, R., Bellion, Y., Benkhelil, J., Moreau, C., 1987. Post Hercynian tectonics in northern and western Africa. Geol. J. 22, 433–466.

Guiraud, R., Bosworth, W., Thierry, J., Delplanque, A., 2005. Phanerozoic geological evolution of northern and central africa: an overview. J. Afr. Earth Sci. 43, 83–143.

Haq, B.U., Hardenbol, J., Vail, P.R., 1987. Chronology of fluctuating sea levels since the triassic. Science 235, 1156–1167.

Harouna, M., Philp, R.P., 2012. Potential petroleum source rocks in the Termit Basin, Niger. J. Petrol. Geol. 35, 165–186.

Head, I., Jones, D., Larter, S., 2003. Biological activity in the deep subsurface and the origin of heavy oil. Nature 426, 344–352.

Hemptinne, J.-C., Peumery, R., Ruffier-Meray, V., Moracchini, G., Naiglin, J., Carpentier, B., Oudin, J.L., Connan, J., 2001. Compositional changes resulting from the water-washing of a petroleum fluid. J. Petrol. Sci. Eng. 29, 39–51.

Horstad, I., Larter, S.R., 1997. Petroleum migration, alteration, and remigration within troll field, Norwegian north sea. AAPG (Am. Assoc. Pet. Geol.) Bull. 81, 222–248.

Hunt, M.J., 1979. Petroleum Geochemistry and Geology. WH Freeman and Company, San Francisco.

Janssen, M., Stephenson, R., Cloetingh, S., 1995. Temporal and spatial correlations between changes in plate motions and the evolution of rifted basins in Africa. GSA (Geol. Soc. Am.) Bull. 107, 1317–1332.

Jones, D.M., Head, I.M., Gray, N.D., Adams, J.J., Rowan, A.K., Aitken, C.M., Bennett, B., Huang, H., Brown, A., Bowler, B.F.J., Oldenburg, T., Erdmann, M., Larter, S.R., 2008. Crude-oil biodegradation via methanogenesis in subsurface petroleum reservoirs. Nature 451, 176–181.

Krumholz, L.R., 2000. Microbial communities in the deep subsurface. Hydrogeol. J. 8, 4–10.

Kuo, L., 1994. An experimental study of crude oil alteration in reservoir rocks by water washing. Org. Geochem. 21, 465–479.

Lai, H., Li, M., Liu, J., Mao, F., Xiao, H., He, W., Yang, L., 2018. Organic geochemical characteristics and depositional models of Upper Cretaceous marine source rocks in the Termit Basin. Niger. Palaeogeogr. Palaeocl. 495, 292–308.

Lai, H., Li, M., Liu, J., Mao, F., Wang, Z., Liu, W., Hong, X., Yang, L., 2019. Source rock assessment within a sequence stratigraphic framework of the Yogou Formation in the Termit Basin, Niger. Geol. J. 55, 2473–2494.

Lai, H., Li, M., Mao, F., Liu, J., Xiao, H., Tang, Y., Shi, S., 2020. Source rock types, distribution and their hydrocarbon generative potential within the Paleogene Sokor-1 and LV formations in Termit Basin, Niger. Energy Explor. Exploit. 1–26, 0.

Larter, S., Wilhelms, A., Head, I., Koopmans, M., Aplin, A., di Primio, R., Zwach, C., Erdmann, M., Telnaes, N., 2003. The controls on the composition of biodegraded oils in the deep subsurface–Part 1: biodegradation rates in petroleum reservoirs. Org. Geochem. 34, 601–613.

Larter, S.R., Adams, J., Gates, I.D., Bennett, B., Huang, H., 2008. The origin, prediction and impact of oil viscosity heterogeneity on the production characteristics of tar sand and heavy oil reservoirs. J. Can. Petrol. Technol. 47, 52–61.

Larter, S.R., Huang, H., Adams, J., Bennett, B., Snowdon, L.R., 2012. A practical biodegradation scale for use in reservoir geochemical studies of biodegraded oils. Org. Geochem. 45, 66–76.

Li, M., Cheng, D., Pan, X., Dou, L., Hou, D., Shi, Q., Wen, Z., Tang, Y., Achal, S., Milovic, M., Tremblay, L., 2010. Characterization of petroleum acids using combined FT–IR, FT–ICR–MS and GC–MS: implications for the origin of high acidity oils in the Muglad Basin. Sudan. Org. Geochem. 41, 959–965.

Li, M., Lai, H., Mao, F., Liu, J., Xiao, H., Tang, Y., 2018. Geochemical assessment of source rock within a stratigraphic geochemical framework: taking Termit Basin (Niger) as an example. Earth Sci. 43, 3603–3615 (in Chinese with English abstract).

Liu, B., Pan, X., Wan, L., Su, Y., Mao, F., Liu, J., Lü, M., Wang, Y., 2012. Structural evolution and main controlling factors of the Paleogene hydrocarbon accumulation in Termit Basin, eastern Niger. Acta Pet. Sin. 33, 394–403 (in Chinese with English abstract).

Liu, J., Zhang, G., Li, Z., Tang, Y., Xiao, H., Lai, H., Yang, C., 2019. Oil charge history of paleogene-eocene reservoir in the Termit Basin (Niger). Aust. J. Earth Sci. 66, 597–606.

Lü, M., Xue, L., Wan, L., Mao, F., Liu, J., Liu, B., Wang, Y., 2015. Main controlling factors of Paleogene hydrocarbon accumulation of Termit Basin, West African rift system. Earth Sci. Front. 22, 207–216 (in Chinese with English abstract).

Lü, X., Wang, Y., Yu, H., Bai, Z., 2017. Major factors affecting the closure of marine carbonate caprock and their quantitative evaluation: a case study of Ordovician rocks on the northern slope of the Tazhong uplift in the Tarim Basin, western China. Mar. Petrol. Geol. 83, 231–245.

Luo, P., Gu, Y., 2005. Effects of asphaltene content and solvent concentration on heavy-oil viscosity. SPE/PS–CIM/CHOA international thermal operations and heavy oil symposium. Calgary 1–3. November. 1–7.

Luo, P., Gu, Y., 2007. Effects of asphaltene content on the heavy oil viscosity at different temperatures. Fuel 86, 1069–1078.

Mao, F., Liu, B., Liu, J., Jiang, H., Yuan, S., Zheng, F., Li, Z., Wang, Y., 2019. The reservoir characteristics and controlling factors of the Upper Cretaceous sandstone in the Termit Basin, Niger. Acta Petrol. Sin. 35, 1257–1268 (in Chinese with English abstract).

Maurin, J.C., Guiraud, R., 1993. Basement control in the development of the early cretaceous west and central African Rift system. Tectonophysics 228, 81–95.

McCaffrey, M.A., Legarre, H.A., Johnson, S.J., 1996. Using biomarkers to improve heavy oil reservoir management; an example from the Cymric Field, Kern County, California. AAPG (Am. Assoc. Pet. Geol.) Bull. 80, 898–913.

Milner, C.W.D., Rogers, M.A., Evans, C.R., 1977. Petroleum transformations in reservoirs. J. Geochem. Explor. 7, 101–153.

Palmer, S.E., 1984. Effect of water washing on C15+ hydrocarbon fraction of crude oils from northwest palawan, Philippines. AAPG (Am. Assoc. Pet. Geol.) Bull. 68, 137–149.

Palmer, S.E., 1993. Effect of biodegradation and water washing on crude oil composition. Org. Geochem. 23, 511–533.

Peters, K.E., Walters, C.C., Moldowan, J.M., 2005. The Biomarker Guide: Biomarkers and Isotopes in Petroleum Exploration and Early History. Seconded, vol. 2. Cambridge University Press, Cambridge.

Price, L.C., 1980. Crude oil degradation as an explanation of the depth rule. Chem. Geol. 28, 1–30.

Qian, K., Robbins, W.K., Hughey, C.A., Cooper, H.J., Rodgers, R.P., Marshall, A.G., 2001. Resolution and identification of element compositions for more than 3000 crude acids in heavy petroleum by negative-Ion microelectrospray high-field Fourier transform ion cyclotron resonance mass spectrometry. Energy Fuel. 15, 1505–1511.

Reyment, R.A., Dingle, R.V., 1987. Palaeogeography of africa during the cretaceous period. Palaeogeogr. Palaeocl. 59, 93–116.

Rubinstein, I., Strausz, O.P., Spyckerelle, C., Crawford, R.J., Westlake, D.W.S., 1977. The origin of the oil sand bitumens of Alberta: a chemical and a microbiological simulation study. Geochem. Cosmochim. Acta 41, 1341–1353.

Seifert, W.K., Moldowan, J.M., 1979. The effect of biodegradation on steranes and terpanes in crude oil. Geochem. Cosmochim. Acta 43, 111–126.

Seifert, W.K., Moldowan, J.M., Demaison, G.J., 1984. Source correlation of biodegraded oils. Org. Geochem. 6, 633–643.

Shanmugam, G., 1985. Significance of coniferous rain forests and related organic matter in generating commercial quantities of oil, Gippsland Basin, Australia. AAPG (Am. Assoc. Pet. Geol.) Bull. 69, 1241–1254.

Stahl, W.J., 1980. Compositional changes and 13C/12C fractionations during the degradation of hydrocarbons by bacteria. Geochem. Cosmochim. Acta 44, 1903–1907.

Tang, G., Sun, Z., Su, J., Tang, X., 2015. Study of Cretaceous sequential stratigraphy and sedimentary system in Termit Basin of west Africa. China Petroleum Exploration 20, 81–88 (in Chinese with English abstract).

Tissot, B., Welte, D.H., 1984. Geochemical Fossils and Their Significance in Petroleum Formation, Petroleum Formation and Occurrence. Springer, Berlin, pp. 93–130.

Tomczyk, N.A., Winans, R.E., Shinn, J.H., Robinson, R.C., 2001. On the nature and origin of acidic species in petroleum. 1. Detailed Acid type distribution in a California crude oil. Energy Fuel. 15, 1498–1504.

Volkman, J.K., Alexander, R., Kagi, R.I., Woodhouse, G.W., 1983. Demethylated hopanes in crude oils and their applications in petroleum geochemistry. Geochem. Cosmochim. Acta 47, 785–794.

Wan, L., Liu, J., Mao, F., Lü, M., Liu, B., 2014. The petroleum geochemistry of the Termit Basin, eastern Niger. Mar. Petrol. Geol. 51, 167–183.

Watson, J.S., Jones, D.M., Swannell, R.P.J., van Duin, A.C.T., 2002. Formation of carboxylic acids during aerobic biodegradation of crude oil and evidence of microbial oxidation of hopanes. Org. Geochem. 33, 1153–1169.

Wenger, L.M., Davis, C.L., Isaksen, G.H., 2002. Multiple controls on petroleum biodegradation and impact on oil quality. SPE Reservoir Eval. Eng. 5, 375–383.

Winters, J.C., Williams, J.A., 1969. Microbiological alteration of crude oil in the reservoir. Amer. Chem. Soc. Div. Petrol. Chem. New York Mtg. Preprints E22–E33.

Xiao, H., Wang, T.-G., Li, M., Lai, H., Liu, J., Mao, F., Tang, Y., 2019. Geochemical characteristic of Cretaceous Yogou Formation source rocks and oil-source correlation within a sequence stratigraphic framework in the Termit Basin, Niger. J. Petrol. Sci. Eng. 172, 360–372.

Yang, F., Wang, T., Li, M., 2015. The distribution of triaromatic steroids and oil group classification of Ordovician petroleum systems in the Cratonic region of the Tarim Basin, NW China. Petrol. Sci. Technol. 33, 1794–1800.

Yang, Z., Li, M., Cheng, D., Xiao, H., Lai, H., Chen, Q., 2018. Geochemistry and possible origins of biodegraded oils in the Cretaceous reservoir of the Muglad Basin and their application in hydrocarbon exploration. J. Petrol. Sci. Eng. 173, 889–898.

Zhang, B., Li, M., Zhao, Q., Wang, T., Zhang, K., Xiao, Z., Huang, S., 2016. Determining the relative abundance of C26–C28 triaromatic steroids in crude oils and its application in petroleum geochemistry. Exp. Pet. Geol. 38, 692–697 (in Chinese with English abstract).

Zhang, Y., Wang, Q., Wang, F., Lu, H., Cui, H., 2016b. Characteristics and control factors of biodegradation of crude oil in L16-A and L16-B structures of Bohai Sea. J. Yangtze Univ. 13, 13–17 (in Chinese with English abstract).

Ziegler, P.A., 1990. Geological Atlas of Western and Central Europe. Shell Internationale Petroleum Maatschappij. B.V, The Hague.